UPPSALA
UNIVERSITET

UPTEC X 13 013
Examensarbete 30 hp
Juni 2013

Quantification of lipid accumulation in the diaphragm after mechanical ventilation

Johan Petersson

UPPSALA UNIVERSITET

Molecular Biotechnology Programme

Uppsala University School of Engineering

UPTEC X 13 013	**Date of issue 2013-06**

Author

Johan Petersson

Title (English)

Quantification of lipid accumulation in the diaphragm after mechanical ventilation

Title (Swedish)

Abstract

During mechanical ventilation the diaphragm experiences an extreme case of muscle unloading. In many cases this results in respiratory muscle dysfunctions making it difficult to wean the patient off the ventilator. One component in this dysfunction is the accumulation of intramyocellular lipids (IMCL) in the diaphragm muscle fibres. Using Oil Red O stainings and confocal microscopy on rat diaphragm sections we have quantified this process. The results show a sudden increase in IMCL contents between 18 and 24 hours. No significant difference between fibre types could be seen.

Keywords

Mechanical ventilation, intramyocellular lipid accumulation, diaphragm, rat, Sprague-Dawely

Supervisors

Lars Larsson
Uppsala Universitet

Scientific reviewer

Carolina Wählby
Uppsala Universitet

Project name	Sponsors
Language **English**	Security
ISSN 1401-2138	Classification
Supplementary bibliographical information	Pages **25**

Biology Education Centre Biomedical Center Husargatan 3 Uppsala
Box 592 S-75124 Uppsala Tel +46 (0)18 4710000 Fax +46 (0)18 471 4687

Quantification of lipid accumulation in the diaphragm after mechanical ventilation

Johan Petersson

Populärvetenskaplig sammanfattning

Mekanisk ventilering, det som i vardagligt tal kallas respiratorvård, är en vanlig behandlingsstrategi på intensivvårdsavdelningar. Genom att rytmiskt blåsa ner en blandning av syrgas och luft i patientens lungor kan man ge konstgjord andning när patientens egen förmåga att andas är nedsatt eller helt saknas.

Vår andningsmuskel diafragman är byggd för att vara aktiv dygnet runt hela livet. Vid mekanisk ventilering är diafragman inaktiv på ett sätt som den inte är gjord för att kunna hantera. Precis som andra muskler försvagas diafragman av att vara inaktiv vilket ofta leder till problem när patienten ska vänjas av från ventilatorn.

I samband med att diafragman försvagas lagras det in fett i cellerna i form av små droppar. Orsaken till detta är inte helt känd men man misstänker att det har att göra med att diafragman får mer energi än den kan använda. I det här arbetet har jag försökt ta reda på hur fort inlagringen sker från det att diafragman blivit inaktiv och hur mycket fett som lagras in. Genom att studera diafragmaprover från råttor som ventilerats mellan 6 timmar och 9,5 dygn med hjälp av respirator har vi sett att mängden fett ligger stabilt fram till och med 18 timmar. Mellan 18 och 24 timmar ökar mängden med runt 10 gånger och håller sig sedan ganska stabilt till 4,5 dygn där det sakta börjar gå ner igen.

Vidare studier krävs för att bekräfta resultaten i denna studie. Förhoppningsvis kan de leda till större förståelse för hur diafragmaskador uppstår under mekanisk ventilering och hur de kan förhindras eller lindras.

Examensarbete 30 hp

Civilingenjörsprogrammet Molekylär Bioteknik

Uppsala Universitet, juni 2013

Table of Contents

Abbreviations

ATP	Adenosine triphosphate
FISH	Fluorescent in situ hybridization
ICU	Intensive care unit
IMCL	Intramyocellular lipid(s)
MND	Myonuclear domain
MV	Mechanical ventilation
MyHC	Myosin heavy chain
ROS	Reactive oxygen species

Introduction

The human body contains a large amount of fat. It is estimated that a healthy male of 70 kg has around 15 kg of triglycerides in his adipose (fat) tissue (Borgström *et. al.* 2013). However, a smaller amount is stored within the skeletal muscle fibres as small lipid droplets (Shaw *et. al.* 2007). These intramyocellular lipids (IMCL) act as an energy reserve during muscle activity (Shaw *et. al.* 2007) and are also connected to the development of type II diabetes in obese patients (Shaw *et. al.* 2007, He *et. al.* 2004).

The number and size of the droplets are believed to be influenced by factors such as age (Shaw *et. al.* 2007), weight and physical fitness (He *et. al.* 2004, Goodpaster *et. al.* 2000). Aging, obesity and low physical fitness are correlated with increased amounts of IMCL. High physical fitness is also correlated to increased IMCL, but the droplets are smaller, more numerous and to a greater degree positioned near the mitochondria, suggesting that they are optimized for the task of serving as energy reserves during physical activity (Goodpaster *et. al.* 2000, He *et. al.* 2004, Shaw *et. al.* 2007).

Muscle unloading and inactivity causes lipid contents to increase (Picard *et. al.* 2012). This happens irregardless of the reason for unloading and there are many similarities between humans and rats. For example, spaceflight, bed rest and limb suspension create similar responses both within and between the two species (Stein & Wade 2005).

A case of extreme muscle unloading can be observed in sedated or pharmacologically paralyzed mechanically ventilated (MV) intensive care unit (ICU) patients, i.e., a treatment strategy during which a patient receives mechanical aid to breath. MV is a frequently used intervention in ICUs. While useful to save the lives of patients suffering from conditions causing reduced or non-existent respiratory capacity, it often turns out to be difficult to wean the patient of the ventilator. One highly important contributor to these problems is respiratory muscle dysfunction that develops during the MV intervention and makes it difficult or impossible for the patient to survive without the machine (Picard *et. al.* 2012). These problems are time consuming to cure and causes additional suffering and increased healthcare costs.

Skeletal muscle fibres in mammals can be broadly divided into type I and type II fibres (also called slow and fast or red and white fibres). Type II can be further divided into IIa, IIx and IIb (although IIb is not detectable in humans) (Renaud 2013). Type I fibres have a smaller cross-sectional area (thus being generally weaker), slower shortening velocity, higher mitochondrial density and greater endurance than type II fibres. Within the fast fibre types, type IIa is the most “type I-like”, IIx is in between and IIb the most “type II-like” (Qaisar 2012). According to earlier studies the IMCL content is affected by fibre type in limb muscles with type I fibres having a higher IMCL content (Koopman *et. al.* 2001, Malenfant *et. al.* 2001).

The diaphragm is a muscle built for constant activity. During controlled MV the diaphragm experiences an unusual situation where it is only exposed to an external load induced by the ventilator but no internal strain induced by the activation of contractile proteins. This causes a wide array of problems such as loss of enzymes involved in the mitochondrial respiratory chain, mitochondrial genome damage, insulin resistance and an accumulation of IMCL in the form of increased size of the IMCL droplets (Picard *et. al.* 2012). Picard and co-workers speculated that the mechanisms underlying their observations were related to a sudden decrease in energy demands

causing an increased production of reactive oxygen species (ROS) damaging mitochondrial DNA. To mitigate the damage caused by the ROS the cell down regulates mitochondrial biogenesis and induces insulin resistance to decrease the influx of energy into the cell (Picard *et. al.* 2012).

While Picard *et. al.* (2012) could see an accumulation of IMCL after a few hours, lab technician Yvette Hedström noticed a clear accumulation in rats who had been MV for several days. This became the basis of the current study.

Aim of the study

Since the accumulation of IMCL in the diaphragm during MV appears to be closely connected to the weaning problems often encountered after MV treatment it's important to study it in greater detail. While there are qualitative observations of IMCL accumulation in the diaphragm after MV, there does not appear to be a quantitative measurement to determine when, how fast and how much the IMCL content increases. Making such a measurement is the aim of this study.

Overview of the experimental procedure

To study the IMCL accumulation we have stained diaphragm tissue sections for lipids using Oil Red O. The tissue sections were taken from rats that had been mechanically ventilated between 6 hours and 9.5 days. Sham-operated rats were used as controls. The stained sections were imaged in a confocal microscope, compared with myosin ATPase stained sections to determine fibre type and analyzed on a single cell basis for lipid content.

Materials and methods

Animals

12 female Sprague-Dawley rats, 2 sham-operated and 10 anaesthetized and mechanically ventilated, were included in the study. The rats were ventilated for durations between 6 and 228 hours. (See table 1.) The experimental model is described in detail by Ochala *et. al*. (2012). In short, the rats were anaesthetized with Isoflurane, pharmacologically neuromusculary blocked with α-cobratoxin and kept mechanically ventilated using a coaxial tracheal cannula. During the experiment the arterial blood pressure, heart rate (ECG), brain activity (by subcutaneous EEG needle electrodes), body temperature, urine output and blood oxygenation were continuously monitored. Animals were kept in protein and fluid balance. Body temperature was servo-regulated at 37°C.

The sham-operated controls underwent the same surgical procedures. They were not pharmacologically neuromusculary blocked and breathed spontaneously until they were killed within 2 hours after initial anaesthesia.

Table 1. The number of animals used for each time point in the study.

Duration of mechanical ventilation (hours)	Number of animals
0	2
6	1
18	2
24	1
32	2
60	1
108	1
180	1
228	1

Sample preparation and staining

Sample preparation

Serial cross-sections on glass slides, 10 µm thick, of rat diaphragm were prepared for each animal and stored at -74°C. For each animal 8 slides containing 2 sections per slide were prepared.

Oil Red O staining

Samples were removed from the freezer and allowed to thaw for 5 minutes in room temperature. A few drops of 3.7% formaldehyde solution were then added to each slide and left to incubate for 1 hour. The slides were moved to glass containers and washed 3 times 30 seconds in deionized water. The containers were then filled with Oil Red O working solution and left to incubate for 30 minutes. The Oil Red O working solution was prepared fresh from 60 ml stock solution and 40 ml deionized water per 100 ml and filtered through VWR brand filter paper (FILTER PAPER QUALITATIVE 413 100/PK) before use. The stock solution was made by adding 2.5 g Oil Red O to 500 ml 60% triethyl phosphate. After pouring of the working solution, the slides were washed 3 times 30 seconds

in deionized water and then rinsed under running tap water for 5 minutes. The slides were carefully wiped off, mounted with 10% glycerol and stored at 4°C.

All Oil Red O staining were done in two baths simultaneously using Oil Red O working solution from the same preparation. Confocal microscopy pictures were taken within 3 days of staining.

Myosin ATPase stainings

Alkaline preincubation (pH 10.3)

The slides were thawed for 20 minutes at room temperature and moved to a glass container. The slides were incubated in alkaline incubation buffer set to pH 10.30 in a 37°C waterbath for 9 minutes. (Alkaline incubation buffer was made by mixing 2.253 g glycin, 2.4 g $CaCl_2$ and 1.755 g NaCl into 300 ml filtered water and adding 270 ml 0.1 mol/l NaOH. pH was adjusted using HCl / NaOH.) The slides were rinsed 3 times in filtered water and then incubated in alkaline incubation buffer with ATP (0.204 g ATP in 120 ml alkaline incubation buffer) set to pH 9.4. Again the 37°C waterbath was used. The slides were rinsed, incubated for 3 minutes at room temperature in 1% $CaCl_2$, rinsed, incubated for 2 minutes at room temperature in 2% $CoCl_2$, rinsed and incubated for 1 minute in 1% $(NH_4)_2S$. The slides were rinsed 4 times, left to dry for 1 hour, mounted with glycerol gelatine and stored at 4°C.

Acidic preincubation (pH 4.3)

The slides were thawed for 20 minutes at room temperature and moved to a glass container. The slides were incubated in acidic incubation buffer set to pH 4.30 in a 37°C waterbath for 5 minutes. (Acidic incubation buffer were made by mixing 3.90 g sodium acetate and 3.7 g KCl into 500 ml filtered water. pH were adjusted using HAc.) The slides were rinsed 3 times in filtered water and then incubated in alkaline incubation buffer with ATP (0.204 g ATP in 120 ml alkaline incubation buffer) set to pH 9.4. Again the 37°C waterbath was used. The rest of the protocol proceeded exactly like in the alkaline preincubation protocol above.

Acidic preincubation (pH 4.5)

The slides were thawed for 20 minutes at room temperature and moved to a glass container. The slides were incubated in acidic incubation buffer set to pH 4.49 (pH 4.48-4.50 acceptable range) in a 37°C waterbath for 5 minutes and 5 seconds. (See previous paragraph.) The slides were rinsed 10 times in filtered water and then incubated in alkaline incubation buffer with ATP (0.204 g ATP in 120 ml alkaline incubation buffer) set to pH 9.4. Again the 37°C waterbath was used. The slides were rinsed twice, incubated for 3 minutes at room temperature in 1% $CaCl_2$, rinsed, incubated for 2 minutes at room temperature in 2% $CoCl_2$, rinsed 3 times and incubated for 1 minute in 1% $(NH_4)_2S$. The slides were rinsed 6 times, left to dry for 1 hour, mounted with glycerol gelatine and stored at 4°C.

Image capture

Confocal microscope images capture

Each Oil Red O stained slide was evaluated and 5 different areas were scanned in sections of highest quality. A Carl Zeiss Laser LSM 510 Meta scanning microscope was used with a C-Apochromat 40x/1.2 W corr water immersion objective, a 633 nm 5.0 mW HeNe laser at 12% output and a LP560 filter for the image capture. Detector settings were detector gain = 429, amplifier offset = -0.015, amplifier gain = 1.14. Image size was 230.5µmx230.5µm at a resolution of 1812x1812. Number of images in each stack varied due to occasional local variations in section thickness at the imaged area (due to folds in or damage to the sections). Those parts of the stacks were omitted from further analysis.

Regular light microscope images capture

All stained slides were photographed in a regular microscope using an Olympus DP11 Microscope Digital Camera System at 10x magnification to facilitate fibre type identification.

Image analysis

Fibre type identification

For identification of fibre types Photoscape version 3.6.3 was used. Confocal images were fitted onto the regular light microscopy images of the Oil Red O stained sections. The images of the myosin ATPase stained sections from the same animal were then overlaid on top which allowed fibre types in the confocal images to be determined.

Quantification in Imaris

For quantification Imaris® version 5.7.2 was used. Single cells were isolated using the contour surface function and the rest of the image was masked. Next, the spots function was used to provide seed points for the region growing function. Parameters for the spots function were spot minimum diameter = 1.00 µm, background subtraction on and spot quality threshold = 500. Region growing were done by source channel with source channel threshold = 2000, removal of overlapping spots and radius from region volume.

For each animal a total of 30 cells were analyzed. With two exceptions 15 cells of type I and 15 cells of type II were picked. (For 6 hours 20 type II and 10 type I cells were analyzed. For 180 hours 17 type II and 13 type I cells were analyzed. In both cases this was done due to a shortage of acceptable type I cells in the stacks.)

Data management and statistical analysis

Volume of a single cell "slice" was calculated by multiplying cell area by 10 µm (section thickness); next total signal volume in each cell was divided by slice volume to get the proportion of signal. The data were log-transformed in order to achieve normal distribution. Next, the procedure PROC RSREG

in SAS® statistical software was used to determine whether a linear or quadratic function best fits the data.

Table 2. PROC RSREG output for the combined data set. The quadratic model is clearly superior to the linear one in this case.

Regression	**DF**	**Type I Sum of Squares**	**R-Square**	**F Value**	**Pr > F**
Linear	1	4.1	0.026	7.19	0.0080
Quadratic	1	59	0.37	103.63	<.0001
Crossproduct	0	0	0.0	.	.
Total Model	2	63	0.39	55.41	<.0001

As evident from Table 2 the quadratic model is the best fit for the data. Using the same procedure on one cell type at a time showed that the signal proportion peaked at different time points.

The data were then analyzed using PROC GENMOD (also SAS®), picking normal distribution for the response data. This was done for each time point separately to compare the two cell types.

It was apparent from the data that the increase in lipids was very rapid, so the first 5 data points were analyzed by a transition function using TableCurve®. The function used was intercept form 8082.

Results

A comment on signal strengths versus IMCL contents

Since we didn't have any absolute standard to compare the results to in this study the signal strength should *not* be directly interpreted as percentages of the cell occupied by Oil Red O stained lipids. The signal strength presented is an arbitrary unit dependent on microscope settings and Imaris® parameter values. The data show only relative increases and decreases in IMCL amounts, not absolute values.

IMCL accumulation over time

Figure 1 shows the signal proportion at different time points. As is evident from the figure there are no significant change in IMCL amounts during the first 18 hours. Between 18 and 24 hours the IMCL increase rapidly and drastically. It then stays relatively stable until somewhere between 108 and 180 hours were it slowly starts to decrease. The pattern remains when calculating signal proportions in the cell types separately. (Figure 2.)

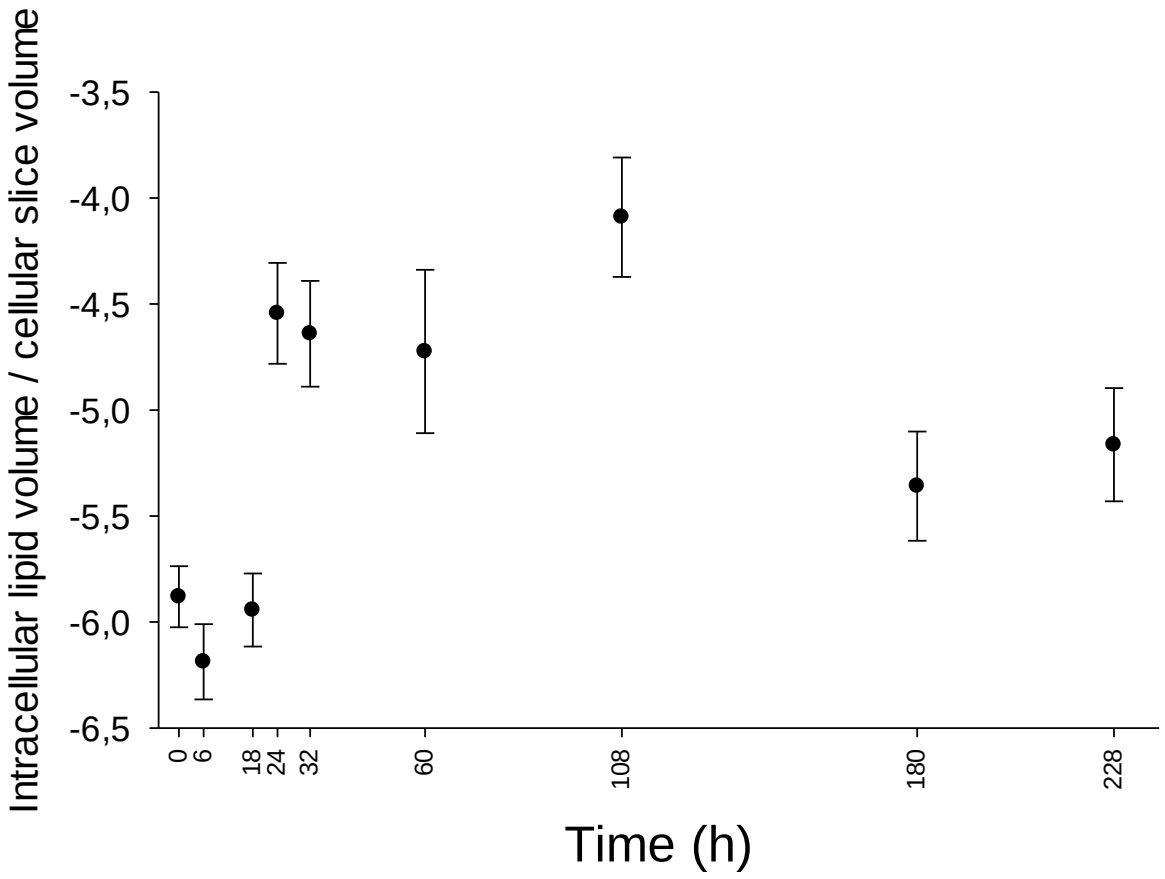

Figure 1. Lipid volume fractions at each time point, log-transformed. Bars show 95% confidence intervals.

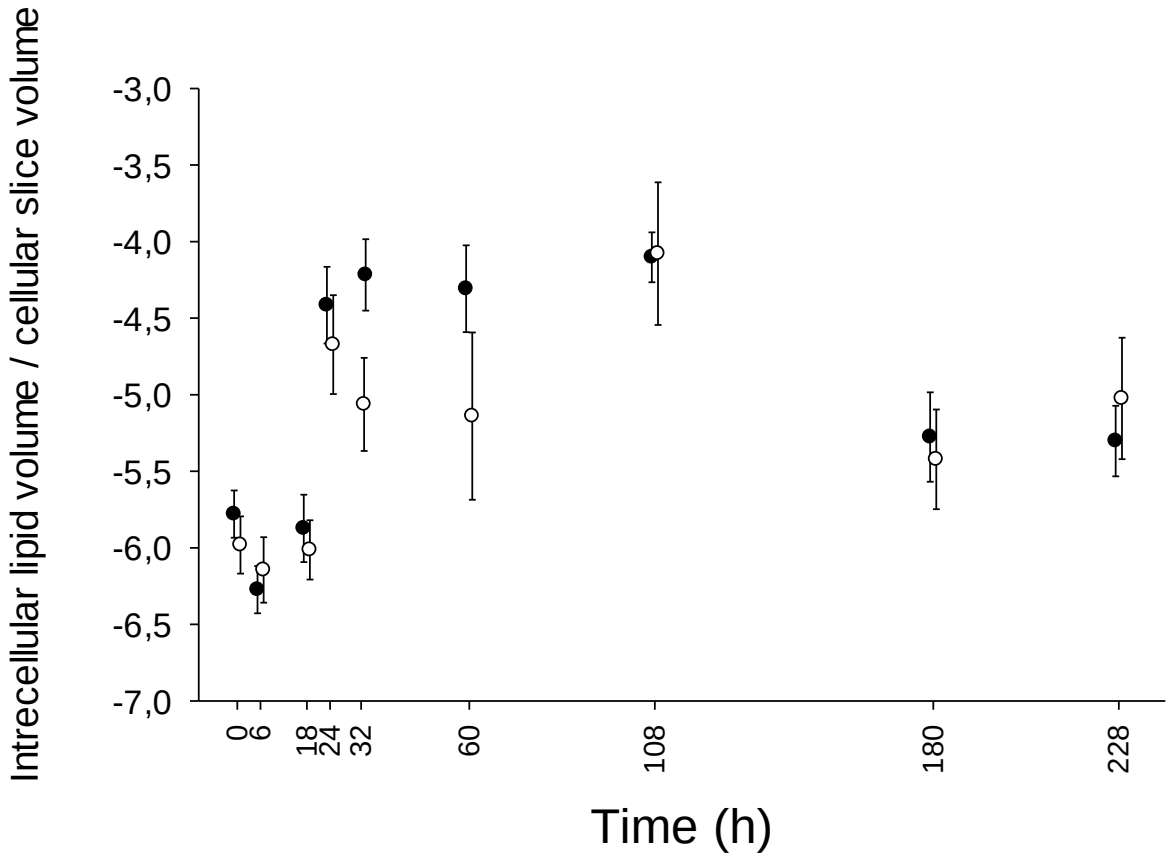

Figure 2. Lipid volume fractions at each time point, log-transformed and calculated for each cell type separately. Black dots are type I fibres, white dots are type II. Bars show 95% confidence intervals. The dots are slightly staggered for ease of view.

A closer look at the difference between cell types

According to earlier studies in limb muscles, type I and type II fibres should have different IMCL content. During normal conditions type I cells have a higher IMCL content. (Koopman *et. al*, Malenfant *et. al*) In the diaphragm muscle fibres in this study, on the other , similar IMCL content was observed in type I and II fibres in control fibres. After 32 and 60 hours of MV, a significantly higher IMCL contents was observed in type I muscle fibres. However, the biological significance of this finding is not clear and it cannot be excluded that this represents a bias since no significant difference in IMCL content was observed at any of the other durations of MV (Figure 2 and Table 3).

Table 3. At which time points do the cell types show significantly different signal strengths? A z value >|1.96| (roughly) indicates significant difference. The AIC value measures how well the model describes the data. (A smaller value indicates a better fit.) z values for whether the signal for the given cell type is significantly different from 0 is given for comparison. Only at T = 32 and T = 60 are the cell types significantly different.

	z value (Signal significantly different from zero?)		**Significant difference between cell types?**		
Time (hours)	**Type I**	**Type II**	**z value**	**Adjusted p value**	**AIC value**
0	-58.32	-60.35	1.44	0.1526	102.9576
6	-42.83	-59.32	-0.72	0.4754	44.9606
18	-49.00	-50.17	0.83	0.4099	125.7782
24	-27.90	-29.54	1.15	0.2481	61.7542
32	-26.89	-32.28	3.81	<0.0001	158.0545
60	-18.04	-21.53	2.46	0.0144	86.4461
108	-21.44	-21.31	-0.09	0.9291	73.1600
180	-28.20	-33.14	0.59	0.5566	67.5279
228	-29.81	-28.25	-1.10	0.2664	68.7721

Peak values

Since the data can be fitted to a quadratic function it is of interest to know when and where it peaks. The peak for type I lie a little higher than the peak of type II as expected since the data set for type I has slightly higher averages.

Table 4. Predicted values and times for the stationary points of the fitted quadratic functions calculated from the different data sets.

Data set	**Time of predicted peak (hours)**	**Value at predicted peak**
Type I	115	-3.96
Type II	128	-4.47
Combined	120	-4.22

The transition function

There is an abrupt increase in IMCL content independent of muscle fibre type early during MV (Figure 1 and 2). To study this transition in more detail, a transition function was fitted to the first 5 time points. The transition width is 20 minutes (0.3362 hours), beginning at 18.35 hours, indicating that this is a fast process.

Figure 3 also illustrates the spread of the data. Each circle represents a single cell. At all time points there are several cells with low IMCL amounts, but the “middle ground” is pushed upwards after the transition.

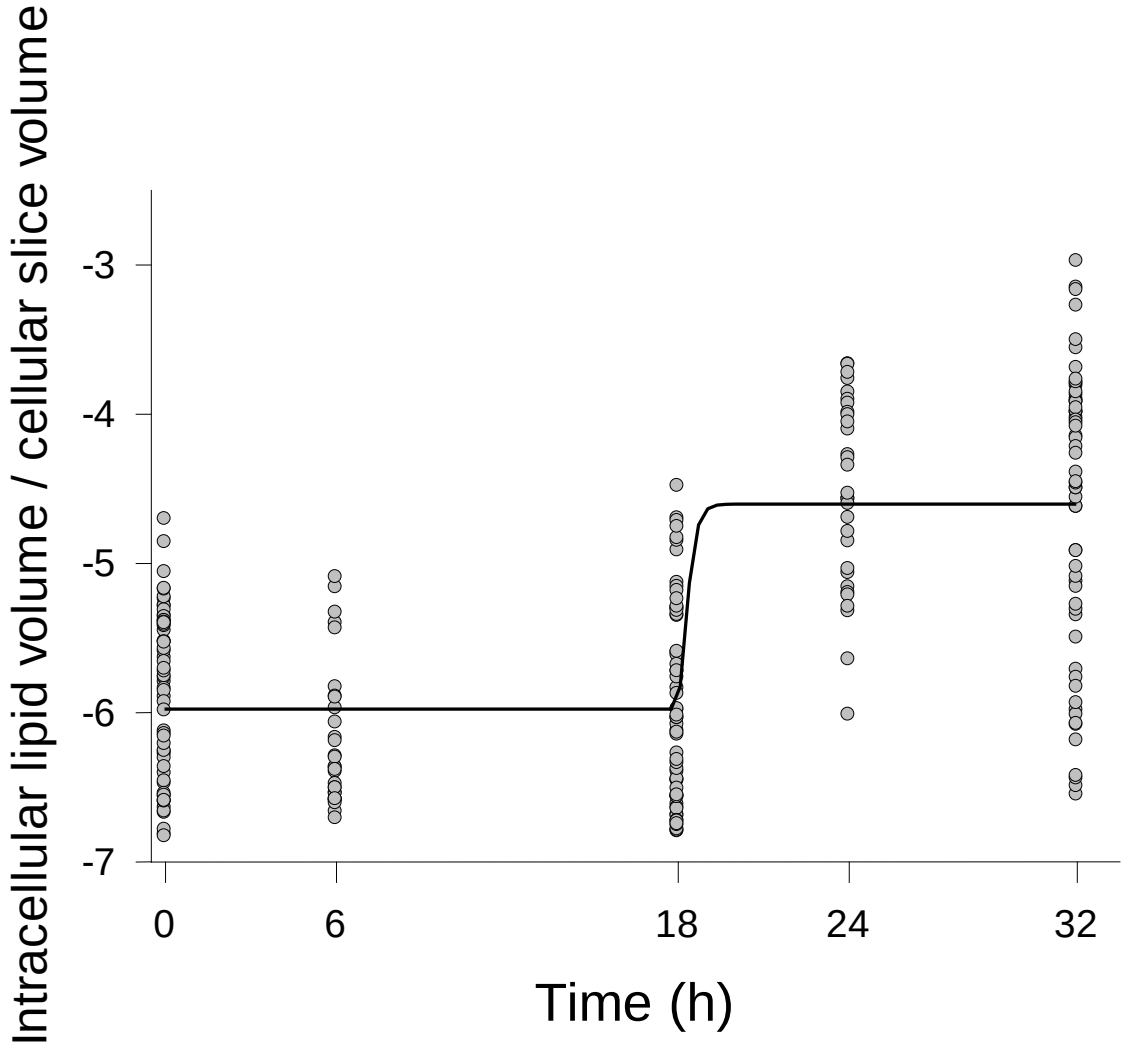

Figure 3. Log-transformed data from the first 5 time points fitted to a transition function. Each circle represents a single cell.

Light microscopy images

Figure 4 illustrates the change in IMCL content. In controls (figure 4A) and after 6 hours (figure 4B) in the ventilator only minor lipid accumulation is visible. At 24 hours (figure 4C) the detected amount has increased noticeably, followed by a levelling off and there was no significant increase in IMCL content after 32 hours (figure 4D).

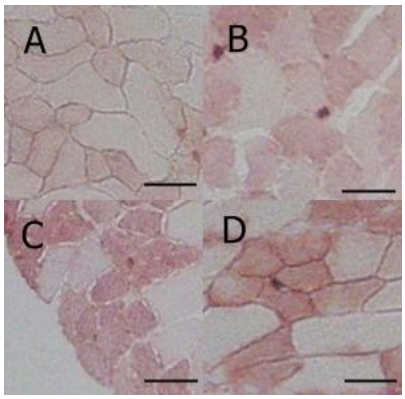

Figure 4. Representative light microscopy images of Oil Red O stained sections photographed at 10x magnification. Time points are 0 hours (A), 6 hours (B), 24 hours (C) and 32 hours (D). Scale bar = 50 µm.

Discussion

Speed, magnitude and pattern of the IMCL accumulation

One previous study has documented an accumulation of IMCL in response to MV in human organ donors. This study aimed to investigate lipid accumulation in an experimental ICU model allowing time-resolved analyses with a high temporal resolution in animals with no underlying disease. The results from this study shows a significant and early increase in IMCL content in response with a transition point between 18 and 24 hours of MV. At 18 hours the IMCL content is at the level of the controls. At 24 hours the IMCL content has increased 10-fold. The lipid accumulation then proceeds at a slower rate, possibly halting entirely, until somewhere between 108 and 180 hours where it begins to decline.

The mechanism underlying the increase at 18-24 hours is not known. Picard *et. al.* (2012) could observe a reduction of diaphragmatic contractile force and an increase in oxidative stress after just 6 hours of MV in mice. However, commercially available ventilators can typically maintain small rodents alive for no more than 12-24 hours, adding a significant confounding factor since the animals are in the process of dying during the entire experiment. The experimental animal model used in this study allows detailed time-resolved studies for several weeks/months. The longest duration a rat has been monitored MV and pharmacologically ventilated is 96 days.

The decrease at the higher time points is also of interest. The total daily caloric intake of the rats in this study were approximately 8 kcal/day (Ochala *et. al*. 2011) during the MV period, far below the maintenance needs of around 45 kcal/day for a female Sprague-Dawley rat of 300 g. (Keenan *et. al.* 1997) Considering that, it is possible that the IMCL were requisitioned for energy in other tissues.

Differences between fibre types

Earlier studies have found that IMCL is higher in type I fibres than in type II fibres (Koopman *et. al.* 2001, Malenfant *et. al.* 2001). This is not unexpected since type I fibres have a high capacity to oxidize lipids (Koopman *et. al.* 2001). This study could not find any significant differences between the fibre types at 0 hours. However, the studies mentioned above were done on limb muscles. It might be possible that the diaphragm differs in how IMCL are stored, considering that the diaphragm (contrary to the limb muscles) are designed to be active more or less constantly.

At two time points (32 and 60 hours) are the fibre types significantly different. In both cases are the type I fibres the ones with the greater signal. At 0, 18 and 24 hours are the average value for type I are noticeably higher, although not significantly so.

In this study I noticed that highly stained cells sometimes lay close together in small clumps consisting of half a dozen cells. (See figure 4D.) By studying cells in close proximity to each other it is possible that highly stained cells of one type were picked disproportionally often in some animals. Since fibres within a given fibre type or at a single time point show a very large variation (see Figure 3) it is possible that a difference between fibre types were missed due to the small sample size in the study. However, this appears to be a less likely mechanism since the lack of a fibre type specific

difference remained if all samples were pooled together. Thus, a muscle specific difference appears more plausible.

The transition

The transition between low and high IMCL is fast and according to the transition function it starts at ~18.5 hours and is finished 20 minutes later. Neither the data set nor the analysis supports making any definitive claims about the exact initiation or the exact time span for the change, but it does indicate that the process starts shortly after the 18 hour mark and finishes before the 24 hour mark. Additional experiments on rats ventilated for between 19 and 23 hours may shed some further light on this process.

Comments on the method

Oil Red O primarily binds to neutral lipids such as triglycerides (Koopman *et. al.* 2001). However, it might also bind to phospholipids in mitochondrial membranes (Jones 2008). This might induce errors in the data; especially when comparing fibre types since type I fibres contain more mitochondria than type II fibres. Its effect on the more general increase in signal is probably less noticeable. During MV mitochondria are lost in the diaphragm (Picard *et. al.* 2012), meaning that the increase in signal might have been even greater if the experiment had been corrected for this. It is possible that an IMCL increase early in the process may have been missed due to mitochondrial loss balancing out an increased IMCL, but the lack of data on the exact magnitude of mitochondrial loss make it difficult/impossible to speculate on this at the moment. Mitochondrial stainings done in parallel to Oil Red O stainings could give valuable insight in this matter.

Not all stained sections made it through the entire process. In addition to the animals listed in Table 1, one additional animal was stained successfully for each of the time points 0, 6, 180 and 228 hours. These showed nearly identical average signal strengths (measured for entire stacks rather than single cells) as the ones included for the same time points. They were excluded from the final analysis due to problems with identifying fibre types.

Conclusions

The present study shows an increase in IMCL accumulation in rat diaphragm after 18-24 hours of mechanical ventilation. No significant differences between fibre types could be identified, but the limited data set could be the reason for that. Additional studies are needed to verify the novel time-resolved results from this study and determine the mechanism underlying the abrupt increase in IMCL content in diaphragm fibres. It is suggested that markers for oxidative stress and mitochondrial function is monitored during these early critical time points.

Acknowledgements

Lars Larsson – First of all I would like to thank my supervisor Professor Lars Larsson for letting me work in his group, for being unceasingly enthusiastic, positive and helpful. I am also grateful for his foresight in having a backup project prepared from the very start and being forthright about the original project.

Carolina Wählby – I want to thank my scientific reviewer Carolina Wählby for taking on the job and for giving valuable advice on the image and data analysis.

Johan Lindqvist and Rebecca Corpeno – For helping me find the right literature to read, for helping me modify the FISH protocols, for teaching me how to use the confocal microscope, for keeping an eye on me and countless other things.

Ann-Marie Gustafson – For answering my endless questions and explaining lots and lots of things about the lab and the group.

Yvette Hedström – For showing and explaining the staining protocols to me and helping me perform them. For teaching me how to use a cryostat, for doing all the paperwork around ordering chemicals, for checking and evaluating the quality of my sections and stainings, for helping me with lots and lots of tiny but important things in the lab and much more. I also want to thank Yvette for noticing and bringing attention to the IMCL accumulation in MV rats that became the basis for this project.

The rest of the people in the research group – Hazem Akkad, Nicola Cacciani, Meishan Li, Hannah Ogilvie and Rutger Norbart for being universally friendly and welcoming.

Erik Petersson – I want to thank my dad for patiently helping me with the statistics and explaining it to me. I also want to thank him for his help in making the figures good and proper.

Lars-Göran Josefsson – Finally, I want to thank my examiner Lars-Göran for taking the project switch in stride and for quickly answering all my questions before and during the project.

References

Borgström Bengt, Fänge Ragnar, Sternby Nils-Herman, Malmquist Jörgen. fettvävnad. http://www.ne.se/lang/fettvävnad, Nationalencyklopedin. Acquired 2013-05-10.

Goodpaster Bret H., Theriault Remy, Watkins Simon C., Kelley David E. 2000. Intramuscular Lipid Content Is Increased in Obesity and Decreased by Weight Loss. Metabolism 49:467-472

He Jing, Goodpaster Bret H., Kelley David E. 2004. Effects of Weight Loss and Physical Activity on Muscle Lipid Content and Droplet Size. Obesity Research 12:761-769

Jones Lamar M. 2008. Lipids. Bancroft John D., Gamble Marilyn. Theory and Practice of Histological Techniques, 6th edition. p187-216. Elsevier Limited. China

Karlsson Edlund Patrick. 2008. Methods and models for 2D and 3D image analysis in microscopy, in particular for the study of muscle cells. Acta Universitatis Upsaliensis. Uppsala

Keenan Kevin P., Ballam Gordon C., Dixit Rakesh, Soper Keith A., Laroque Philippe, Mattson Britta A., Adams Stephen P., Coleman John B. 1997. The Effects of Diet, Overfeeding and Moderate Dietary Restriction on Sprague-Dawley Rat Survival, Disease and Toxicology. Journal of Nutrition 127(5):851S-856S

Koopman René, Schaart Gert, Hesselink Matthijs K.C. 2001. Optimisation of oil red O staining permits combination with immunofluorescence and automated quantification of lipids. Histochemistry and Cell Biology 116:63-68

Lea Robert, Bonev Boyan, Dubaissi Eamon, Vize Peter D., Papalopulu Nancy. 2012. Multicolor Fluorescent In Situ mRNA Hybridization (FISH) on Whole Mounts and Sections. Hoppler Stefan, Vize Peter D. (editors). Xenopus Protocols: Post-Genomic Approaches, Second Edition. pages 431-444. Humana Press, New York

Malenfant Patrick, Joanisse Denis R., Thériault Remy, Goodpaster Bret H., Kelley David E., Simoneau Jean-Aimé. 2001. Fat content in individual muscle fibers of lean and obese subjects. International Journal of Obesity 25:1316-1321

Newlands Sarah, Levitt Linda K., Robinson Stephen C., Karpf Carmen A.B., Hodgson Vanessa R.M., Wade Robert P., Hardeman Edna C. 2012. Transcription occurs in pulses in muscle fibers. Genes & Development 12:2748-2758

Ochala Julien, Gustafson Ann-Marie, Llano Diez Monica, Renaud Guillaume, Li Meishan, Aare Sudhakar, Qaisar Rizwan, Banduseela Varuna C., Hedström Yvette, Tang Xiaorui, Dworkin Barry, Ford Charles G., Nair Sreekumaran K., Perera Sue, Gautel Mathias, Larsson Lars. 2011. Preferential skeletal muscle myosin loss in response to mechanical silencing in a novel rat intensive care unit model: underlying mechanisms. Journal of Physiology 589(Part 8):2007-2026

Picard Martin, Jung Boris, Liang Feng, Azuelos Ilan, Hussain Sabah, Goldberg Peter, Godin Richard, Danialou Gawiyou, Chaturvedi Rakesh, Rygiel Karolina, Matecki Stefan, Jaber Samir, Des Rosiers Christine, Karpati George, Ferri Lorenzo, Burelle Yan, Turnbull Douglass M., Taivassalo Tanja, Petrof

Basil J. 2012. Mitochondrial Dysfunction and Lipid Accumulation in the Human Diaphragm during Mechanical Ventilation. American Journal of Respiratory and Critical Care Medicine 186:1140-1149

Qaisar Rizwan. 2012. Myonuclear Organization and Regulation of Muscle Contraction in Single Muscle Fibres. Acta Universitatis Upsaliensis. Uppsala

Renaud Guillaume. 2013. Intensive care Muscle Wasting and Weakness. Acta Universitatis Upsaliensis. Uppsala

Shaw Christopher S., Jones David A., Wagenmakers Anton J. M. 2007. Network distribution of mitochondria and lipid droplets in human muscle fibres. Histochemistry and Cell Biology 129:65-72

Stein T. Peter, Wade Charles E. 2005. Metabolic Consequences of Muscle Disuse and Atrophy. Journal of Nutrition 135(7):1824S-1828S

Youn Min-Young, Takada Ichiro, Imai Yuuki, Yasuda Hisataka, Kato Shigeaki. 2010. Transcriptionally active nuclei are selective in mature multinucleated osteoclasts. Genes to Cells 15:1025-1035

Appendix

The original project (*Analysis of the spatial organization of transcriptional activity in individual myonuclei along the length of individual skeletal muscle cells*)

The original plan for this project was that I would do a study on myonuclear domains (MND) and patterns of transcriptional activity in individual myonuclei along the length of the muscle cells. Due to experimental difficulties this project did not work out and I moved to the IMCL-project. However, in the interest of accounting for what I did during the first 2.5 months of my project time I will make a short report on this work.

Background

A skeletal muscle cell is one of the two known types of truly multinucleated cell types in the human body, the other being osteoclasts (Youn *et. al.* 2010). Each differentiated skeletal muscle cell (or myofiber) contains hundreds or thousands or nuclei (Qaisar 2012). Together they supply the cell with the mRNA required to produce the proteins necessary for the cell's functions. The nuclei (called myonuclei) seem to occupy fixed and non-random positions in the cell, probably to optimize transportation of proteins and RNA (Qaisar 2012). The different myonuclei differ somewhat in what proteins they produce. For example, myonuclei close to a myotendineus junction (an interface with a tendon) produce specific proteins required in that area (Qaisar 2012). The nuclei also differ in their transcriptional activity. While all nuclei are transcriptionally *competent*, they are not all transcriptionally *active* simultaneously (Newlands *et. al.* 2012). Further, each locus appears to be independently regulated and transcription occurs in pulses – not continuously even though the protein products are continuously present (Newlands *et. al.* 2012).

Aim of the study

The aim of the study was to study the pattern of transcriptional activity in myofibers, i.e. how are transcriptional activity distributed in 3 dimensions in the cell?

Overview of the experimental procedure

We used fluorescent in situ hybridization (FISH) with cDNA probes targeted against a sequence in the myosin heavy chain (MyHC) mRNA. The same sections were then stained with DAPI to visualize nuclei and the sections where analyzed using confocal microscopy. By studying which nuclei had mRNA around them and which did not, one could be able to study the pattern of transcriptional activity.

Materials and Methods

Sample preparation

10 µm thick cross sections and longitudinal sections were prepared from right medial quadriceps muscle from rat.

cDNA probe

MyHC was picked as the target for the probe because it is the most highly expressed protein in myofibers. By using NCBI and BLAST a 29 base pair sequence in the rat MyHC mRNA:s was found that are identical in all fibre types (I, IIa, IIx, IIb). The final probe sequence were: TCCTTCTTGTACTCCTCCTGCTCCAGCAC

The probe was ordered from Thermo Fisher Scientific with a 5' ATTO 610 fluorescent tag.

FISH

The protocol used is a modified version of "Method for Fluorescent In Situ Hybridization on Cryosections" presented by Lea *et. al*. (2012). All solutions used up until the addition of the hybridization buffer were autoclaved before use and prepared under RNAse free conditions. Additionally, the stock solutions for PBS and SSC were autoclaved before use. Slides were left to dry at room temperature for 1 hour, then transferred to a glass beaker filled with 1x PBS + 0.1% Triton for 2 minutes. 250 µl 0.1 M TEA were pipetted on to each slide. After 15 minutes the slides were placed in a glass beaker and washed 2 times 5 minutes with 1x PBS + 0.1% Tween-20. 500 µl 4% formaldehyde in 1x PBS 0.1% Tween-20 were added to each slide. After 15 minutes 750 µl prewarmed hybridization buffer (50% formamide, 0.1% Tween-20 and 100 µg/ml heparin in 5x SSC) was pipetted on to each slide, they were placed in a plastic hybridization chamber with wet tissue on the bottom and incubated for 2 hours at 60°C. The hybridization buffer were tipped off and replaced with 1 µg/ml probe in hybridization buffer. A coverslip was added and the slides incubated over night at 60°C.

The slides were carefully dipped in 2x SSC to remove the coverslip, then incubated in 2x SSC for 10 minutes at room temperature. 500 µl wash buffer (50% formamide and 0.05% Tween-20 in 2x SSC) were added to each slide and they were incubated for 30 minutes at 60°C. Slides were then washed 2 times 15 minutes in 2x SSC at 60°C, 2 times 15 minutes in 0.2x SSC at 60°C, once for 10 minutes in 1x TBSTw (100 mM TRIS 7.5, 150 mM NaCl, 0.05% Tween-20) at room temperature and once for 20 minutes in 3% H_2O_2 diluted in 1x TBSTw room temperature. The edges of the slides were wiped carefully, a line was drawn around the edges with a PAP pen and 150 µl blocking solution (1% Heat Treated Lamb Serum and 0.5% Blocking medium made from Roche® Blocking Reagent in 1x TBSTw) were added. The slides were incubated for 1 hour at room temperature, washed 3 times 10 minutes in 1x TBSTw and mounted using Duolink II mounting medium with DAPI.

Confocal microscopy

Several different settings were tried for the microscope.

Results and comments

Sectioning, fixation and DAPI staining worked without problems. The sections looked fine and the DAPI stained nuclei were clearly visible, but the probe turned out to be problematic. We could see only very faint signals from the probe channel and signals were clustered in small clumps, seemingly randomly dispersed across the slide with nearly equal amounts on and off the sections. We added additional washing steps which removed the probe signal clumps but did nothing else. We tried to modify incubation times, decrease oven temperature from 60°C to 50°C, decreasing the number of washes or using mounting mediums without DAPI. We compared sections without probe, sections with probe and sections with probe at 5 times recommended concentrations, all done using the same steps at the same time but in different baths. No difference in the signal could be seen. Clean slides with only a drop of water, mounting medium and coverslip showed signal strengths almost as high as the others.

I am still unsure exactly why this method did not work, but there are a host of possible reasons. Due to the results when using blank slides without sections it is possible that the background from what little ambient light (mostly from the computer screen) there were in the dark microscope room were enough to drown out the signal completely. I tried to turn off the screen when scanning and that noticeably reduced the signal. It is possible that a single probe molecule per mRNA created a signal that was too weak to be detected. Using probes targeted to different parts of the same mRNA or targeted to a repeating sequence might have solved the problem. However, it is also likely that the problem lies earlier in the protocol. The protocol was originally designed for non-fluorescent probes (using antibodies to provide signal) and it is possible that while partially redesigning the protocol to accommodate our fluorescent probe some fatal errors were made. A few components that appeared to be non-essential (judging from comparing this FISH protocol with others) were omitted from the recipe for the hybridization buffer since they were too expensive to justify buying for such a short project. (Considering that FISH is not a technique often used in this laboratory excess materials would go to waste.) That could be at least part of the cause of the problems. It is also possible that despite the care taken to keep the first steps RNAse free the mRNAs in the sections might have been degraded before the completion of the fixation. There could also be some problems with the sections or tissue samples. The problem might lie with the mRNA. It is possible that the secondary structure of the MyHC mRNAs doesn't allow access to the target sequence. We checked predicted secondary structures, but the MyHC mRNAs are large and difficult to fold in its entirety. Finally, the probe itself might be the problem. Maybe it forms some form of secondary structure that the secondary structure prediction algorithms did not pick up. It is also possible that the sequence of the probe were incorrect, despite my efforts to ensure the opposite.